Experimental and numerical crashworthiness investigation of hybrid composite aluminum tubes under dynamic axial and oblique loadings

H. R. Zarei

Aeronautical University of Science and Technology, Tehran, Iran.

Abstract

This research deals with axial and oblique impact crash tests on simple and hybrid composite tubes. Axial and oblique impact tests have been generated on simple and hybrid composite tubes with one, two and three layers. A drop test rig was used to conduct the experiments. Furthermore, in order to gain more detailed knowledge about the crash process, finite element simulations of the experiments have been performed. The explicit finite element code LS-DYNA was used. The simple tube and the composite hybrid tubes are modeled with thin layer shell elements. The elastic-plastic material model was used for the aluminum tube and the Chang-Chang failure model was implemented for the composite layers. In terms of finding more efficient (higher energy absorption) and lighter crash absorbers particularly, the absorbed energy E and specific energy absorption SAE are considered in this research.

Keywords: Hybrid tube, Composite, Crashworthiness

During the last decades, large numbers of articles have considered the crash performance of thin-walled metallic columns as well as fiber reinforced composite columns. Metallic and composite columns are used in a broad range of automotive and aerospace applications, especially as crash-absorbing elements. In automotive applications, crashworthy structures absorb impact energy in a controlled manner, thereby bringing the passenger compartment to rest without subjecting the occupant to high decelerations. Metallic crash absorbers normally absorb energy by progressive folding and local bending as the column walls collapse. A distinctive feature of such a deformation mechanism is that the energy dissipation is concentrated over relatively narrow zones, while the remainder of the structure maintains its rigidity.

The crashworthiness of the crash box is expressed in terms of its energy absorption E and specific energy absorption SEA. The energy absorption is equal to the area under the crash load–displacement curve while specific energy absorption is defined as the energy absorption per crushed mass.

Increased interest on vehicle safety has led to a comprehensive research of the crash response of aluminum tubes from several points of view namely, analytical, numerical and experimental. Wierzbicki and Abramowicz [1] presented a simple formula to predict the axial crash behavior based on the balance of external and internal work. This model was validated experimentally by Abramowicz and Jones [2]. Alexander [3], Pugsley [4], Abramowicz [5],Abramowicz and Jones [6], Singac and Elsobky [7] and Wierzbicki and Bhatalso [8] used the same method to predict the crush behavior of circular tubes.

In recent years, Hybrid composite tubes in which metallic tubes are combined with fiber reinforced composites are considered for improving the crush performance of turbular structures. For example, Ragalyi and Mallick [9], Babbage and Mallick [10] produced hybrid tubes containing aluminum tubes and a filament-wound E-glass fiber-reinforced epoxy overwrap. They observed that the hybrid tubes have significantly higher energy absorption than either the composite tubes or the aluminum tubes. Shin et al. [11] performed quasi-static axial crush and bending collapse tests on hybrid tubes produced by wrapping glass fiber/epoxy prepregs around square aluminum tubes and found that for low weight absorbers the hybrid tubes have good energy absorption. In addition to these experimental works, Hanefi and Wierzbicki [12] published an analytical model for the estimation of mean axial crush load of circular metal tubes externally wrapped with hoop wound composite layers. In this model, the fiber orientation in the composite layers was 90o to the tube axis. Mamalis et al. [13, 14] used the explicit FE Code LS-DYNA to simulate the crash behavior and energy absorption of thick-walled square tubular components made of

hybrid sandwich material with corrugated core subjected to axial compressive load. The comparison of their numerical results with actual experimental data from small-scale models in terms of deformation modes, energy absorption capability, load/deflection history and crush zone characteristics, shows very good agreement.

Babbage and Mallick [15] describe an experimental investigation on the static axial crush performance of aluminum–composite hybrid tubes, containing filament-wound E-glass fiber reinforced epoxy over-wrap around aluminum tubes. Both unfilled and foam-filled hybrid tubes were tested. The fiber orientation angle in the overwrap was either ±45 o or ±75 o to the tube axis. Both round and square aluminum tube cross sections were considered. They compared the static axial crush resistances of these tubes in terms of the maximum load, mean crush load, crush energy, specific energy absorption and the deformation mode.

El-Hagel et al. [16] used finite element method to study the quasi-static axial crush behavior of the aluminum composite hybrid tube containing filament-wound E-glass fiber reinforced epoxy over-wrap around an aluminum tube. The fiber orientation angle in the over-wrap was ±45o to the tube axis. A modified Chang–Chang failure model was used for the composite layers.

Greve et al. [17] presented a new simulation technique for phenomenological modeling of stable fragmentation in fiber reinforced composite structures under dynamic compressive loading. They used an explicit crash code for implementation of a hybrid modeling technique, in which two distinct material models act simultaneously. The first model was implemented in a multi-layered shell element and uses a unidirectional composites fracture criterion to predict potential ply fracture mechanisms on a macroscopic scale. This model was, however, unable to represent the complex localized fracture mechanisms that occur on a meso (sub-ply) scale under compression fragmentation loading. Therefore, a second constitutive model was added to capture the energy absorbing process within the fragmentation zone, utilizing an Energy Absorbing Contact (EAC) formulation between the composite structure and the impacting body. They performed a series of dynamic axial and oblique impact tests of cylindrical continuous carbon fiber reinforced composite tubes to validate the approach.

This work deals with experimental and numerical studies on the crash investigation of the simple and hybrid composite tubes containing a square aluminum tube and a fiber reinforced composite overwrap in which the fiber orientation angle is $\pm$ 45o to the tube

axis. Here, several axial and oblique impact tests have been conducted on simple and hybrid composite tubes. Also the explicit finite element code LS-DYNA is used to find more detail about the crash process. The crush performance of simple and hybrid tubes is expressed in terms of their energy absorption and specific energy absorption. Finally the crush behavior of simple and hybrid tubes are compared.

2. Material Properties

The aluminum tubes were made from coustomary quality extruded 6060 aluminum alloy (AlMgSi 0.5F22) in the received treatment conditions. Mechanical properties of the aluminum tube were determined from standard tensile testing of coupons cut from several tubes. The yield stress σ0.2=231 MPa and ultimate stress σult=254 MPa have been determined [18].

The composite layers were made from E-glass fiber and epoxy resin. The laminate thickness and weight were 0.448 mm and 729 g/m2, respectively .

3. Experimental Details

Axial and oblique dynamic crash tests have been conducted on simple and hybrid aluminum square tubes. The outer diameter of the aluminum tubes was 55 mm; while the nominal wall thickness was 2 mm. Tubes with a length of 270 mm was used. The hand layup method has been used to prepare the hybrid tubes. An impact mass of 154 kg was selected for all tests. The tests have been performed to define the strengthening effect of the composite over warp.

The experimental tests were conducted on the drop test rig; see Figure 1a, which is installed at the Institute of Dynamics and Vibrations at the University of Hanover. Figure 1b shows how the specimens were placed under axial and oblique impact conditions. This test rig has a mass which can be varied from 20 to 300 kg; the maximum drop height is 8 m and a maximum impact speed of 12.5 m/s can be reached. The force and displacement are recorded with a PC using AD-converter. The force is measured using strain gauges and a laser displacement sensor provides the axial deformation distance of the tube.

The interest in this study was the mean crushing load P_m and the energy absorption E. The mean crash load is defined by:

$$P_m = \frac{1}{\delta_{Max}} \int_0^{\delta_{Max}} P(\delta)\, d\delta \qquad , \qquad (1)$$

where $P(\delta)$ is the instantaneous crash load corresponding to the instantaneous crash

displacement δ . The area under the crash load displacement curve represents the absorbed energy E.

4. Numerical Simulation

Numerical simulations of crash tests have been performed to obtain local information such as time histories of the stress and strain fields everywhere in the tube, which are difficult to measure during the crash. The modeling and analysis have been performed on a UNIX server using the explicit finite element code LS-DYNA. The simple and hybrid tubes with the dimension of the tested specimens have been considered. Because of the symmetry, only one half of the specimen is modeled. The aluminum tube walls and composite layers are modeled with Belytschko-Tsay thin shell elements. The symmetrical boundary conditions were applied on all free vertical edges. Rigid body elements have been used to model the impactor.

Because initial geometrical imperfections influence strongly the first peak load, initial imperfections have been prescribed along the length and width of the model in the analyses with the following expression [19]:

$$W = w_0 sin(n\pi x / l)Sin(\frac{\pi y}{D-T}) \tag{2}$$

Here D and T are tube width and thickness, respectively and w_0 is the amplitude and n is the number of half-sine waves along the length. In these simulations the parameters were defined by $w_0 = 0.1$ mm and $n = 5$.

The contact between the rigid body and the specimen is modeled using a node to surface algorithm with a friction coefficient of μ=0.2. To account for the contact between the tube walls during deformation, a single surface contact algorithm has been used. To simulate the adhesive bounding, an automatic TIEBREAK contact algorithm was implemented between the composite layers and aluminum tube walls.

The aluminum alloy is modeled as an elastoplastic material using isotropic and kinematic work hardening with the use of material number #103 in LS-DYNA. The strain hardening model used in this material model is described by

$\sigma_e = \sigma_{0.2} + \alpha Q_1[1-\exp(-c_1\varepsilon^p)](1-\alpha)Q_2[1-\exp(-c_2\varepsilon^p)]+\sigma_v.$
(3)

Here, $\sigma_{0.2}$ is the proportional limit in a uniaxial material test; $\varepsilon^p = \varepsilon - \sigma / E$ is the plastic strain; c_i gover the rate of change in the isotropic and kinematic hardening variables; Q_i represent their

asymptotic values; α determines the relationship between isotropic and kinematic hardening; whereas σ_v is the viscous stress. Since the aluminum alloys are strain rate insensitive, see Reyes et al. [20], the viscous effect is neglected in this study.

The load displacement curve has an oscillating behavior due to the formation of lobes. Numerical results of Berstadt et al. [21] have shown that this behavior is associated with loading and unloading of the material and that the relationship between isotropic and kinematic hardening may be important for the energy absorption. The crash responses of tubes with different hardening parameters α are determined in [22]. The result showed that the value of α=1 , i.e. non-linear isotropic hardening, gives a reasonable result.

The impactor is modeled with rigid material. The composite walls are modeled using material model #54 in LS-DYNA. This model has the option of using either the Tsai–Wu failure criterion or the Chang–Chang failure criterion for lamina failure. The Tsai–Wu failure criterion is a quadratic stress-based global failure prediction equation and is relatively simple to use; however, it does not specifically consider the failure modes observed in composite materials [23]. Chang–Chang failure criterion [24] is a modified version of the Hashin failure criterion [25] in which the tensile fiber failure, compressive fiber failure, tensile matrix failure and compressive matrix failure are separately considered. Chang–Chang modified the Hashin equations to include the non-linear shear stress–strain behavior of a composite lamina. They also defined a post-failure degradation rule so that the behavior of the laminate can be analyzed after each successive lamina fails. According to this rule, if fiber breakage and/or matrix shear failure occur in a lamina, both transverse modulus and minor Poisson's ratio are reduced to zero, but the change in longitudinal modulus and shear modulus follows a Weibull distribution. On the other hand, if matrix tensile or compressive failure occurs first, the transverse modulus and minor Poisson's ratio are reduced to zero, while the longitudinal modulus and shear modulus remain unchanged. The failure equations selected for this study are based on the Chang–Chang failure criterion. However, in material model #54, the post-failure conditions are slightly modified from the Chang-Chang conditions. For computational purposes, four indicator functions e_f, e_c, e_m, e_d corresponding to four failure modes are introduced. These failure indicators are based on total failure hypothesis for the laminas, where both the strength and the stiffness are set equal to zero after failure is encountered.

Tensile fiber mode: (fiber rupture)

$$\sigma_{aa} > 0, \text{then } e_f^2 = \left(\frac{\sigma_{aa}}{X_t}\right)^2 + \xi \left(\frac{\sigma_{ab}}{S_c}\right)^2 - 1 \begin{cases} \geq 0 \ failed \\ < 0 \ elastic \end{cases} \quad (4)$$

Where ξ is a weighting factor for the shear term in tensile fiber mode and $0 < \xi < 1.0$.

$E_a = E_b = G_{ab} = v_{ba} = v_{ab} = 0$ after lamina failure by fiber rupture.

Compressive fiber mode: (fiber buckling or kinking)

$$\sigma_{aa} < 0, \text{then } e_c^2 = \left(\frac{\sigma_{aa}}{X_c}\right)^2 - 1 \begin{cases} \geq 0 \ failed \\ < 0 \ elastic \end{cases} \quad (5)$$

$E_a = v_{ba} = v_{ab} = 0$ after lamina failure by fiber buckling or kinking.

Tensile matrix mode: (matrix cracking under transverse tension and in-plane shear)

$$\sigma_{bb} < 0, \text{then } e_m^2 = \left(\frac{\sigma_{bb}}{Y_t}\right)^2 + \left(\frac{\sigma_{ab}}{S_c}\right)^2 - 1 \begin{cases} \geq 0 \ failed \\ < 0 \ elastic \end{cases} \quad (6)$$

$E_b = v_{ba} = 0 \rightarrow G_{ab} = 0$ after lamina failure by matrix cracking.

Compressive matrix mode: (matrix cracking under transverse compression and in-plane shear)

$$\sigma_{bb} < 0, \text{then } e_d^2 = \left(\frac{\sigma_{bb}}{2S_c}\right)^2 + \left[\left(\frac{Y_c}{2S_c}\right)^2 - 1\right]\frac{\sigma_{bb}}{Y_c} + \left(\frac{\sigma_{ab}}{S_c}\right)^2 \begin{cases} \geq 0 \ failed \\ < 0 \ elastic \end{cases} \quad (7)$$

$E_b = v_{ba} = v_{ab} = 0 \rightarrow G_{ab} = 0$ after lamina failure by matrix cracking.

In Equations 4-7, σ_{aa} is the stress in the fiber direction, σ_{bb} is the stress in the transverse direction (normal to the fiber direction) and σ_{ab} is the shear stress in the lamina plane $aa - bb$. The other lamina-level notations in these Equations are as follows:

X_t and X_c are tensile and compressive strengths in the fiber direction, respectively

Y_t and Y_c are tensile and compressive strengths in the matrix direction, respectively

S_c is shear strength

E_a and E_b are Young's modulus in the longitudinal and transverse directions, respectively

v_{ab} and v_{ba} are major and minor Poisson's ratios

G_{ab} is shear modulus

Equations 4-7 are applied for each lamina in a laminate to determine if it has failed. When a lamina fails, the post-failure conditions are applied to that lamina and a ply-discount method is applied to

determine its subsequent contribution to the laminate's load carrying capacity and failure.

5. Results and discussion

The experimental and numerical studies have been conducted on aluminum tubes and hybrid composite tubes containing a square aluminum tube and a fiber reinforced composite overwrap in which the fiber orientation angle is $\pm 45o$ to tube's axis. Axial and oblique impact tests have been conducted on simple and hybrid composite aluminum tubes. Two tests have been performed for each case, for a total of 24 experiments.

The energy absorption and specific energy absorption of the simple and hybrid square aluminum tubes in axial and oblique impact are compared.

5.1 Axial and oblique impact on square aluminum tubes

The results of axial and oblique impact tests on simple square aluminum tubes are shown in Table 1. Here, the tests are named by giving the type of tube, followed by the number of layers of composite material and impact angle, then whether it was the first or second tube tested by A and B letter. Dynamic crush load and displacement were measured in this experiment. Furthermore, the crash performance has been simulated using LS-DYNA explicit code. Figure 2–4 show the experimental and simulated crush load displacement curves of simple tubes under axial and oblique impact tests. A quick observation on numerical crush load displacement curves will indicate that the numerical results are in good agreement with experimental ones. Only the mean crush load in the simulation curve is a little bit higher than experimental results. Therefore, the final crush displacement in simulation is smaller than the experimental results.

In the case of axial impact the curve starts with high peak load that corresponds to elastic-plastic buckling of the tube and continues with a repeated pattern, see Figure 2. Each pair of peaks is related with the creating of one lobe. But in the case of oblique impact, see Figure 3 and 4 and Table 1, the results are different. It can be recognized that the load angle has dramatic influence on the first peak load. When the impact is generated with an angle greater than zero, the first peak decreases. The impact angle has an influence on the mean crush load as well. When the impact angle increases the mean crush load decreases.
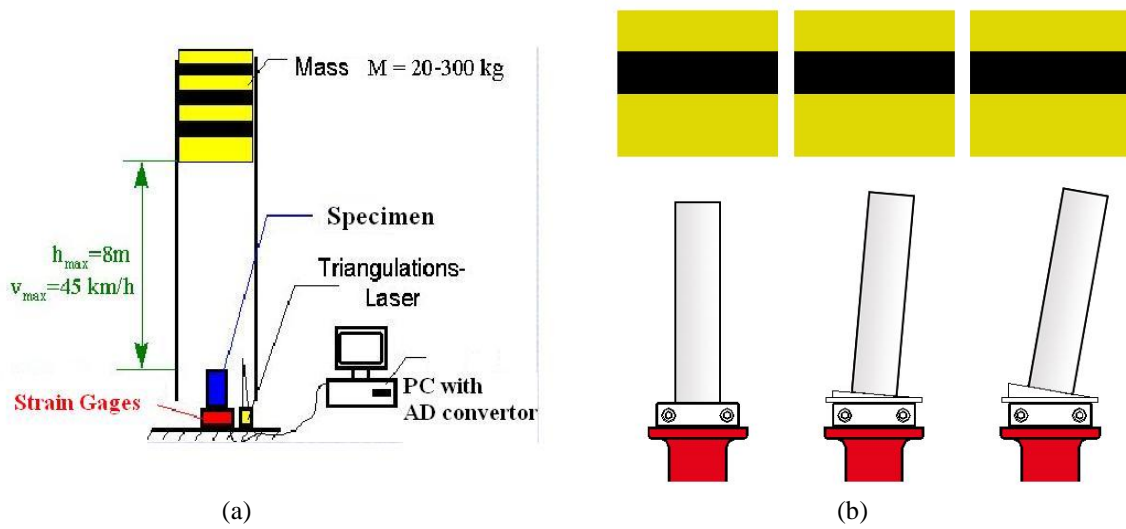
(a)   (b)

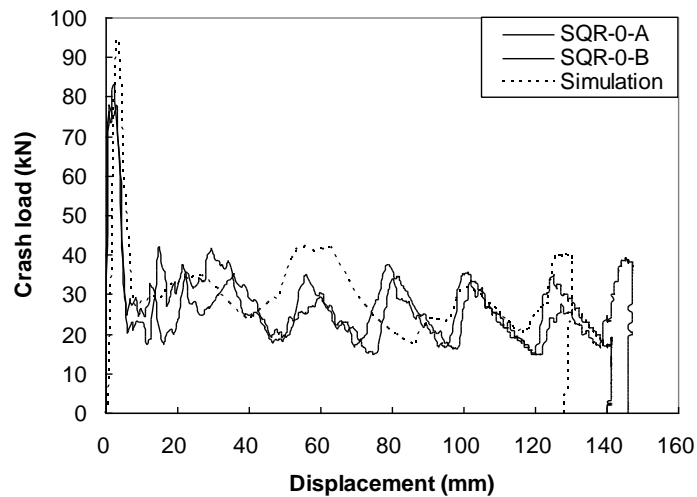**Fig 1**. a) Test setup, b) Specimens in axial and oblique impact conditions.

Fig 2. Experimental and numerical crush load-displacement curve of square aluminum tube for axial crash.
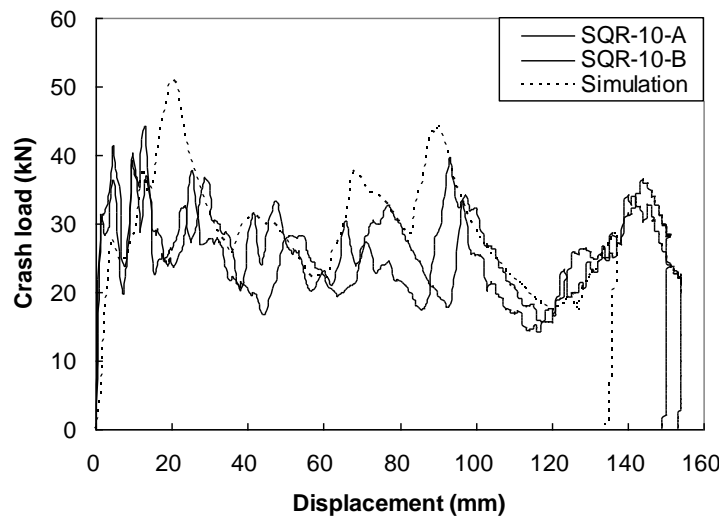
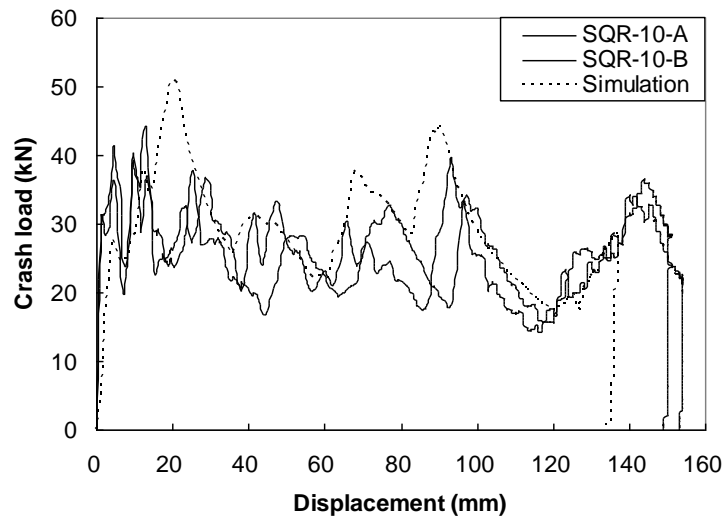**Fig3**. Experimental and numerical crush load-displacement curve of square aluminum for 5o oblique crash

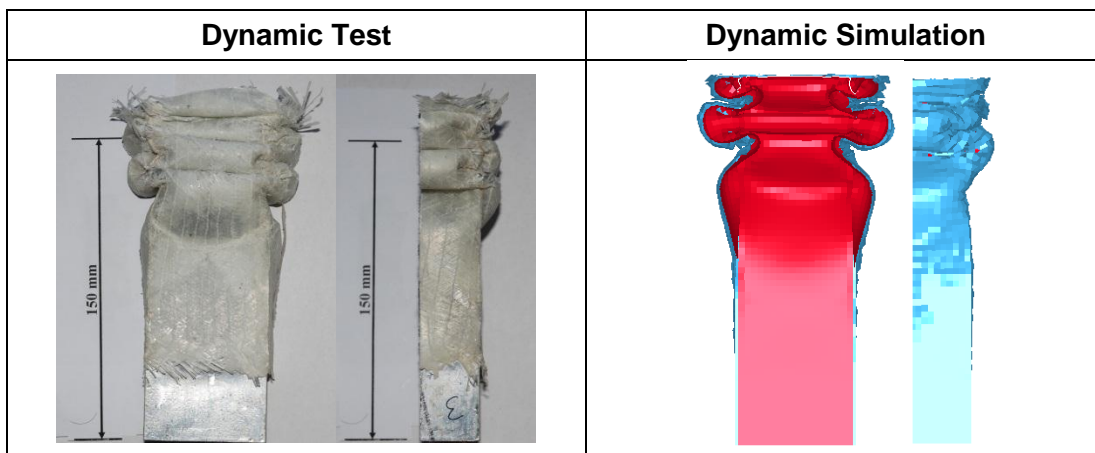**Fig4.** Experimental and numerical crush load-displacement of square aluminum tube for 10o ablique crash.

Fig5. Experimental and numerical crush pattern of one-layered hybrid tube for axial crash.

5.2 Axial and oblique impact on composite hybrid tubes

The results of impacts with different angles on hybrid composite tubes have been generated and are shown in Table 2. Figure 5–10 show the experimental and numerical results of the impact on hybrid tubes. The numerical and experimental crash patterns of one layer hybrid tubes are compared in Figure 5. Here, the number of lobs and deformation modes in numerical and experimental results are the same. Also Figure 6 presents the experimental and numerical crash-load displacement curves for one layer hybrid composite tubes. Again the numerical mean crash load is higher than experimental one. The same results for two and three layers hybrid composite tubes are presented in Figures 7-10. It is

satisfying that the simulations have been nearly verified by experiments.

In oblique impact tests, dramatic decrease in the first peak load can be found again, see the crush load-displacement curve in Figure 8 and 10. The mean crush load level also has been decreased as a result of non-axial impact condition for one layer hybrid tube. From Table 1 and 2 also in Figure 2–10 it can be observed that in the same impact conditions the mean crush loads in composite hybrid tubes are higher than in square aluminum tubes. That means composite hybrid tube has been strengthened in the axial compressive direction. When the aluminum tube starts to deform, the composite layer resists against it and therefore the mean crush load in the hybrid tube is higher than in the simple tube.

Table 3–5 show the absorbed energy and specific absorbed energy of square and hybrid composite

tubes at 100 mm crush displacements that have been extracted from experimental results. To remove noises those occur during the test, experimental data have been filtered. Considerations of the energy absorption and specific energy absorption of one-layered hybrid composite tubes in Table 3 indicate that the composite hybrid tube has considerable effects on the crush behavior of tubes. The increase in energy absorption and specific energy absorption takes place simultaneously in one-layered hybrid tubes. This means that more energy can be absorbed by a lighter structure.

For more than one layer composite material (two- and three layered hybrid tubes), see Table 4 and 5, the crash efficiency (energy absorption) is increasing but the structures lose their weight efficiency. In the two- and three-layered hybrid composite tubes, the composite leaves were separated from the overlap side of the aluminum tube. The high strength of composite layers in comparison with the strength of the adhesion between composite and tube, results in a separation of the composite layers from the tube during the crush process. Therefore the aluminum tube did not have any extra support of composite layer. As a result the energy absorption of the two- and three- layered composite tubes are not as much as expected.
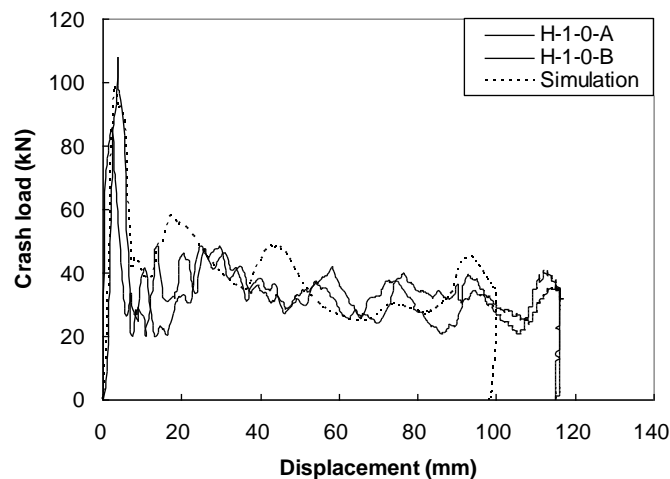

Fig6. Experimental and numerical crush load-displacement curve of one-layered hybrid tube for axial crash.
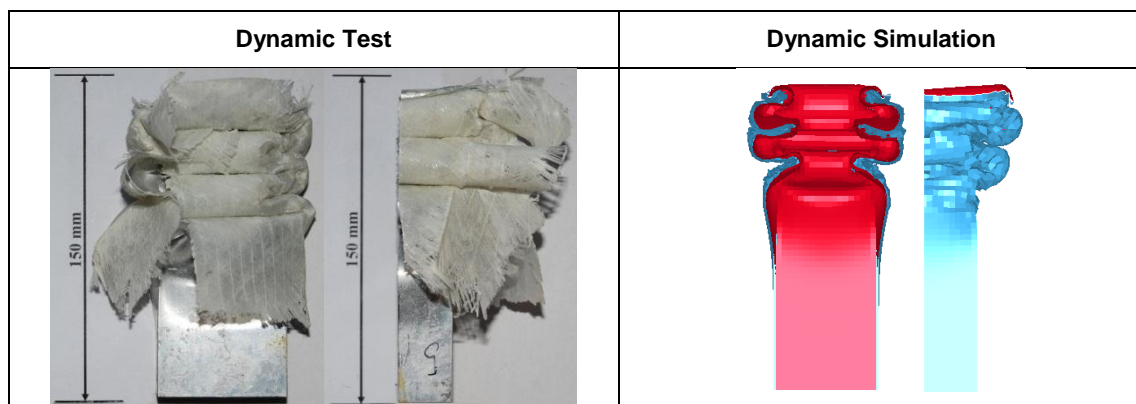
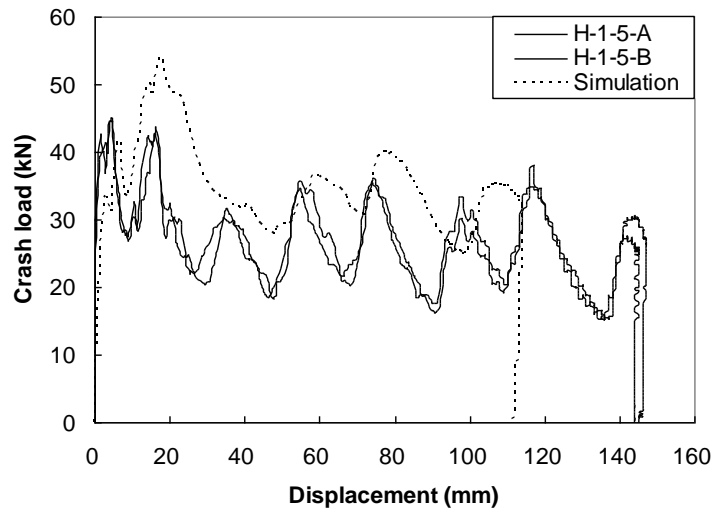**Fig 7.** Experimental and numerical crush pattern of one-layered hybrid tube for 5o oblique crash.

Fig 8. Experimental and numerical crush load-displacement curve of one-layered hybrid tube for 5o oblique crash.

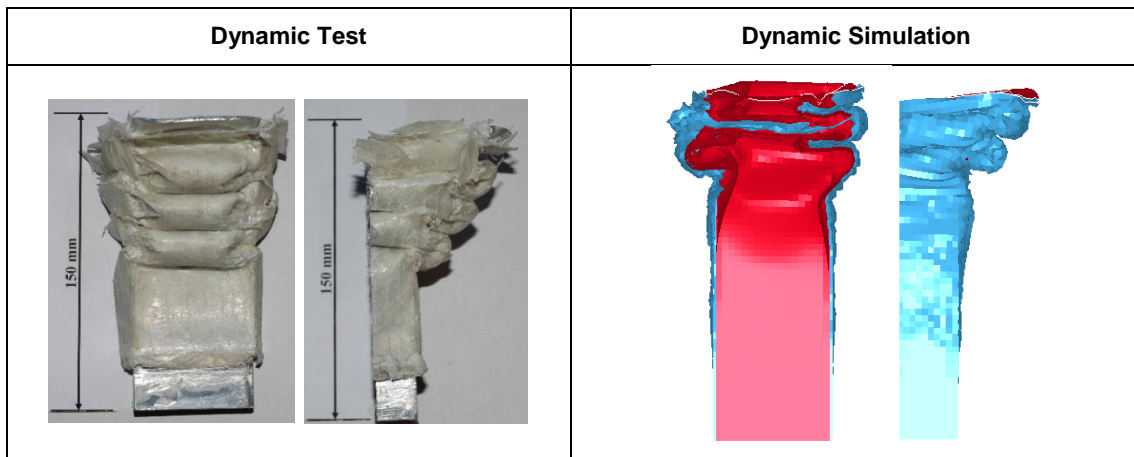| Dynamic Test	Dynamic Simulation

Fig 9. Experimental and numerical crush pattern of one-layered hybrid tube for 5o oblique crash.
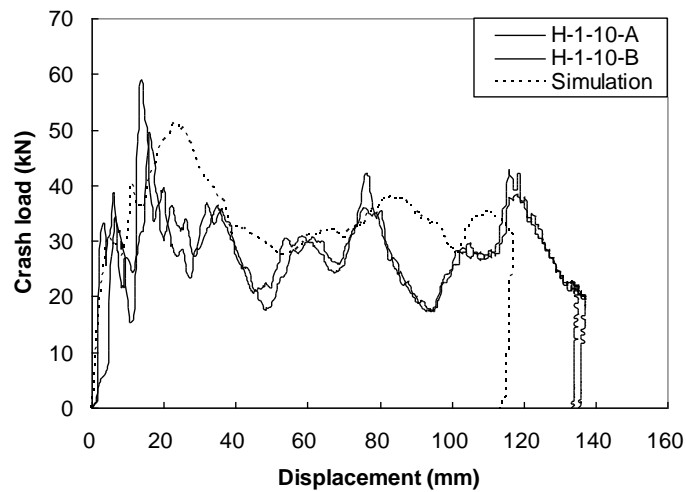

Fig 10. Experimental and numerical crush load-displacement curve of one-layered tube for 10o oblique crash.

CONCLUSIONS

Several axial and oblique impact tests have been generated on simple and hybrid composite tubes. To characterize the crush behavior of the tubes their energy absorption E and specific energy absorption SAE are considered. In order to gain more detailed information about crash behavior, the process was simulated with the explicit finite element code LS-DYNA. Interesting crash characteristics were obtained from the experimental and numerical analysis. Some attractive results are the following:

The experimental crash tests on simple aluminum tubes showed that this structure has good capacity to absorb impact energy.

The oblique impact tests showed that the first peak and mean crush loads are influenced by the impact angle. Lower values were seen in the oblique tests.

The simulated mean crush load of the simple aluminum tube was a little higher than in experiment.

The crush pattern of one layer composite hybrid tubes showed that the tube and composite were not detached from each other and deformed together.

During the experiment, the composite layers in two and three layers hybrid tubes were separated from aluminum tubes.

Considerable increase can be seen in the energy absorption and specific energy absorption of one layer hybrid composite tubes. That means more energy has been absorbed by less weight.

The comparison between the numerical energy absorption and specific energy absorption of the simple tube and hybrid composite tubes with one, two and three layers showed that only in the one layer hybrid tube the energy absorption and specific energy absorption increase simultaneously. In the case of two and three layers composite hybrid tubes, the energy absorptions increase but the specific energy absorption decreases.

References

[1]. Wierzbicki T, Abramowizc W. "On the crashing mechanics of thinwalled structures". J Appl Mech 1983;50:727-39.

[2]. Abramowizc W, Jones N. "Dynamic axial crashing of square tubes". Int J Impact Eng 1984;2:263-81.

[3]. Alexander JM. "An approximate analysis of the collapse of thin cylindrical shells under axial loading". Q J Mech Appl Math 1960;13:10-5.

[4]. Pugsley AG. "On the crumpling of thin tubular structures". Q J Mech Appl Math 1979;32:1-7.

[5]. Abramowizc W, "The effective crushing distance in axially compressed thin-walled metal columns". Int J Impact Eng 1983;1:309-17.

[6]. Abramowizc W, Jones N. "Dynamic axial crashing of square tubes". Int J Impact Eng 1984; 2:179-281.

[7]. Singac AA, Elsobky H. "Further experimental investigation on the essentricity factor in the progressive crushing of tubes". Int J Solids Struct 1996; 32:3589-602.

[8]. Wierzbiki T. Bhat SU. "A moving hinge solution for axisymmetric crushing of tubes. Int J Mech Sci 1986; 28:135-51.

[9]. Ragalyi A, Mallick P K. "Crashworthiness of aluminum-composite hybrid crush tubes containing filament-wound over-wraps" In: Proceedings of SAMPEACCE-DOE-SPE Midwest advanced materials and processing conferences, Dearborn, MI, 2000.

[10]. Babbage J, Mallick P K. "Axial crush resistance of aluminum composite hybrid tubes", Proceedings of 17th annual technical conference of the American society for composites, paper no. 070, 2002.

[11]. Shin K C, Lee J J, Kim K H, Song M C, Huh J S. "Axial crush and bending collapse of an aluminum/GFRP hybrid square tube and its energy absorption capability", Composite struc, 2002;57:279-287.

[12]. Hanefi E H, Wierzbicki T. "Axial crush resistance and energy absorption of externally reinforced metal tubes", Composites: part B, 1996;27B:387-394.

[13]. Mamalis AG, Manolakos DE, Ioannidis MB, Kostazos PK, Papapostolou DP." Axial collapse of hybrid square sandwich composite tubular components with corrugated core: numerical

modeling Composite Structures 58 (2002) 571–582

[14]. Mamalis AG, Manolakos DE, Ioannidis MB, Kostazos PK. "Crushing of hybrid square sandwich composite vehicle hollow bodyshells with reinforced core subjected to axial loading: numerical simulation", Composite Structures 61 (2003) 175–186

[15]. Babbage JM, Mallick PK. "Static axial crush performance of unfilled and foam-filled aluminum–composite hybrid tubes". Composite Structures 70 (2005) 177–184

[16]. El-Hagel H, Mallick PK, Zamani N. "Numerical modeling of quasistatic axial crash of square aluminum-composite hybrid tubes". Int J Crashworthiness 2004;9(6):653–64.

[17]. Greve L , Pickett AK , Payen F. " Experimental testing and phenomenological modeling of the fragmentation process of braided carbon/epoxy composite tubes under axial and oblique impact, Composites: Part B" 39 (2008) 1221–1232

[18]. Zarei H, Kröger M. "Optimum honeycomb filled crash absorber design". J Mater Design, 2006.

[19]. Reyes A, Langseth M, Hopperstad, OS. "Square aluminum tubes subjected to oblique loading". Int J Impact Eng 2003;28:1077-1106

[20]. Reyes A, Langseth M, Hopperstad OS. "Crashworthiness of aluminum extrusions subjected to oblique loading: experiments and numerical analyses". Int J Mech Sci 2002;44:1965-1984.

[21]. Berstad T, Langsrth M, Hopperstad OS. "Crashworthiness of thin- walled aluminum extrusions". 4th Int Conf Comput plast 1995. Barcelona;3-6April

[22]. Zarei H, Kröger M, Popp K. "On the dynamic crash load efficiency of circular aluminum tubes". Sixth Europ Conf Struct Dyna 2005. Paris:4-7sep.

[23]. Mallick PK. "Fiber reinforced composites". 2nd ed. NY: Marcel Dekker; 1990.

[24]. Chang FK, Chang KY. " Post-failure analysis of bolted composite joints in tension and shear-out mode failure". J Compos Mater 1987;21:809–33.

[25]. Hashin Z. " Failure criteria for unidirectional fiber composites". J Appl Mech 1980;47:329–34.